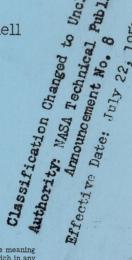# NACA

CASE FILE
COPY

RESEARCH MEMORANDUM

INVESTIGATION AT SUPERSONIC SPEEDS OF EXTERNAL-DRAG

EFFECTS AND PUMPING CHARACTERISTICS

OF A SHORT EJECTOR

By Eugene S. Love and Robert M. O'Donnell

Langley Aeronautical Laboratory
Langley Field, Va.

NATIONAL ADVISORY COMMITTEE
FOR AERONAUTICS

WASHINGTON

June 14, 1955

NATIONAL ADVISORY COMMITTEE FOR AERONAUTICS

RESEARCH MEMORANDUM

INVESTIGATION AT SUPERSONIC SPEEDS OF EXTERNAL-DRAG

EFFECTS AND PUMPING CHARACTERISTICS

OF A SHORT EJECTOR

By Eugene S. Love and Robert M. O'Donnell

SUMMARY

An investigation was conducted at free-stream Mach numbers of 1.62, 1.94, and 2.41 to determine the external-drag effects and pumping characteristics of a short ejector (spacing ratio of 0.19) housed within a highly boattailed afterbody. The tests covered secondary to primary diameter ratios of 1.50 and 1.33, mass flow ratios from 0 to 0.20, and a sonic and a supersonic primary nozzle; the temperature ratio was about one (cold air jet). All tests were conducted with an artificially induced turbulent boundary layer along the model. Jet static-pressure ratios were varied from the jet-off condition to about 36 for the sonic nozzle and to a maximum of about 8 for the supersonic nozzle.

INTRODUCTION

In recent years considerable attention has been given to the effects that a propulsive jet exhausting from the base of a body may have upon the base and afterbody drag of a body at supersonic speeds. Numerous investigations have been made of these effects (see refs. 1 to 15, for example), but relatively few have dealt with combined primary jet flow and secondary or cooling air flow. The pumping characteristics of ejectors exhausting into still air have been fairly well established through investigations of the type reported in references 16 to 22. Although much of this information should be directly applicable, insofar as ejector performance is concerned, to the case of supersonic outer streams of varying Mach number, there are undoubtedly certain critical conditions of operation and of ejector and nozzle geometry for which the Mach number of the external flow would have some effect. These critical conditions are, at present, not clearly defined, and the probable magnitude of the effect when it does occur has not been established.

The investigations reported in references 10 and 11 are examples of recent studies in which afterbody and base pressures, drag, and pumping characteristics have been measured at supersonic speeds for combined primary jet flow and secondary flow. The present investigation is a continuation of a general investigation of the effects of a primary jet (sonic and supersonic nozzle) with and without secondary air flow upon the base and afterbody drag of a body of revolution; pumping characteristics of the ejector are also being measured. The first part of this investigation was reported in reference 11 for the case of a zero-length ejector or zero spacing ratio. (Spacing ratio is defined as the ratio of the distance between the plane of the primary nozzle exit and the plane of the model base to the exit diameter of the primary nozzle.) The results to be presented herein are for the same model but with an ejector having a spacing ratio of about 0.19. Jet static-pressure ratio was varied from the jet-off value to about 36 for the sonic nozzle and to a maximum of about 8 for the supersonic nozzle. As in reference 11 the primary variables were free-stream Mach number, primary jet Mach number, secondary exit area, and the ratio of secondary mass flow to primary mass flow.

SYMBOLS

A area

C_{D_B} base-drag coefficient, $P_B\left(\dfrac{A_N}{A_{max}}\right)$ or $P_B\left(\dfrac{A_B - A_j}{A_{max}}\right)$

C_{D_A} boattail pressure-drag coefficient, $\displaystyle\int_{.82}^{1} P_A \dfrac{d}{d\frac{x}{L}}\left(\dfrac{r}{r_{max}}\right)^2 d\dfrac{x}{L}$

$C_{D_{AB}}$ total afterbody drag coefficient, $C_{D_A} + C_{D_B}$

d diameter

L total body length

M free-stream Mach number

P pressure coefficient, $\dfrac{p - p_\infty}{q_\infty}$

p static pressure

p_0 total pressure

q dynamic pressure

w ratio of mass flow of secondary air to mass
flow of primary jet

x axial distance measured from nose of model

z axial distance measured from base of model

Subscripts:

B base of model

j primary jet

∞ free-stream condition

s secondary flow

A boattail surface

max   maximum value

N base annulus of shroud only

APPARATUS

Wind Tunnel

All tests were conducted in the Langley 9-inch supersonic tunnel which is a continuous-operation, closed-circuit type in which the pressure, temperature, and humidity of the enclosed air can be regulated. Different test Mach numbers are provided by interchangeable nozzle blocks which form test sections approximately 9-inches square. Eleven fine-mesh turbulence damping screens are installed ahead of the supersonic nozzle in a settling chamber of relatively large area. A schlieren optical system is provided for qualitative flow observations.

Model

With the exception of the change in ejector length from 0 to 0.071 inch, the model (see fig. 1) is the same as that employed in

reference 11 and described therein. Two interchangeable afterbodies
or shrouds permit a change in secondary discharge area. Both the
sonic $(M_j = 1)$ and supersonic $(M_j = 3.23)$ nozzles have essentially the
same exit area. Static-pressure orifices are located on the boattail
surface as shown in figure 1, and base-pressure orifices are located at
90° intervals around the annuli of both shrouds with two of the four
orifices in line with the support struts.

TESTS AND PROCEDURE

Tests were conducted at Mach numbers of 1.62, 1.94, and 2.41 with
a stagnation pressure of approximately 1 atmosphere; the corresponding
Reynolds number range, based on body length, was from 2.1×10^6 to
2.9×10^6. All testing was done at 0° angle of attack and with an
artificially induced turbulent boundary layer along the model. The
latter was accomplished by use of a 1/8-inch-wide fine salt band placed
approximately $1\frac{1}{4}$ inches from the model nose. (See fig. 1.)

The afterbody and base pressures were recorded for both shrouds for
the jet-off condition and up to primary jet static-pressure ratios of
about 36 for the sonic nozzle and to about 8 or lower, depending on Mach
number, for the supersonic nozzle. In reference 11, the support struts
were found to have negligible effect on the base pressures, hence an
average value obtained from the four orifices was used in calculating
base drag.

Primary total pressures were measured by means of a calibrated total-
pressure tube within the stagnation chamber ahead of the nozzle as
described in reference 11. Jet static pressures were calculated from the
measured total pressures on the basis of the exit Mach number as deter-
mined from the measured area ratio. Auxiliary tests have shown this pro-
cedure to be reliable. Primary mass flows for both nozzles were calcu-
lated by using the measured total pressure and assuming the nozzle to be
choked at the minimum area. Secondary mass flows of 0 to 20 percent of
the primary mass flow were measured directly by means of calibrated
rotameters.

Throughout the tests the dewpoint of the tunnel air was kept suffi-
ciently low to insure negligible condensation effects. The air supply
for the primary jet and secondary had approximately the same dewpoint as
the tunnel air. The stagnation temperature of the tunnel air was about
100° F, while that for both the primary jet and secondary air was about
80° F (primary to secondary temperature ratio of about 0.96, or essen-
tially unity).

PRECISION

Model alinement was maintained within ±0.1° of zero pitch and yaw with respect to the tunnel center line. Based on past surveys of the stream, the free-stream Mach number is accurate to within ±0.01. The pressure coefficients are accurate to within approximately ±0.003.

Secondary mass-flow ratios are estimated to be within ±0.2 percent, whereas total recorded pressures in the jet model were accurate within ±0.01 inch of mercury for pressures less than 50 pounds per square inch and ±0.5 inch of mercury for higher pressures.

RESULTS AND DISCUSSION

The discussion is presented in two parts: the first part concerning the effects of the primary jet and secondary flow upon drag, and the last, the pumping characteristics. Results for the case of no primary jet flow or secondary flow have been presented in reference 11 and will not be discussed herein except to mention the slight differences in the experimental base and boattail pressures for the two shrouds. These differences were attributed to slightly different external shroud contours and orifice installations. These construction differences were within the machining accuracy of shroud duplication and are not expected to affect the conclusions drawn from the results. In all drag results to be presented, small arrows have been placed on the left-hand ordinates of the figures to indicate the values for jet off and no secondary flow.

Drag

Base drag.- The values of base-drag coefficient C_{D_B} to be presented are the negative products of the average base pressure coefficients and the ratio of base annulus area to maximum body frontal area, $\dfrac{A_N}{A_{max}}$. $\Big($ Negative C_{D_B} implies thrust.$\Big)$ Since this area ratio is 0.100 for the first shroud and 0.1425 for the second shroud, like values of C_{D_B} do not imply like values of P_B.

The variation of C_{D_B} with jet static pressure ratio $\dfrac{p_j}{p_\infty}$ for the sonic nozzle is shown in figure 2(a) for the first shroud $\left(\dfrac{d_s}{d_j} = 1.50\right)$

and in figure 2(b) for the second shroud $\left(\frac{d_s}{d_j} = 1.33\right)$. The general vari-

ation of C_{D_B} with $\frac{p_j}{p_{t\infty}}$ follows what might be expected from previous

investigations of jet effects without secondary flow (see ref. 7, for example). Increasing free-stream Mach number apparently does not alter

significantly the change in C_{D_B} with $\frac{p_j}{p_\infty}$. With some exceptions at the

lower pressure ratios at $M = 1.94$, the effect of mass flow ratio is small.

Figure 3 presents similar results for the supersonic nozzle. Over a comparable range of jet pressure ratio, the effects of increasing mass flow ratio are greater for the supersonic nozzle than for the sonic nozzle at $M = 1.62$ and of the same order at $M = 1.94$ and 2.41. The positive peak occurring in the base-drag curves at the lower pressure ratios is characteristic of primary jet effects; this peak is observed to occur at a lower pressure ratio for the supersonic nozzle and is asso-ciated with the lower pressure ratio for starting for this nozzle. (The term "starting" refers to the theoretical jet static-pressure ratio required to bring a normal shock to the nozzle exit.)

Comparison of the results for the two shrouds gives an indication

of the effects of secondary to primary diameter ratio $\frac{d_s}{d_j}$ for the par-

ticular condition of constant $\frac{p_j}{d_B}$ only since, first, the difference in

annulus area is contained in C_{D_B} and, second, P_B would experience

some effect by the change in $\frac{d_s}{d_B}$. For this condition and taking into

account the jet-off value of C_{D_B} (see arrows on ordinates of figures)

the effect of decreasing $\frac{d_s}{d_j}$ from 1.50 to 1.33 for both the sonic and

supersonic nozzle is small and, for the most part, negligible.

In both figures 2 and 3 dashed curves have been shown that represent C_{D_B} based on a common base annulus area, $A_B - A_j$, for the case of no

secondary flow. Some observers propose that the values of C_{D_B} thus

obtained represent roughly the maximum jet effects upon base drag (the maximum possible base area over which the base pressure may act has been

included) and are therefore useful in preliminary estimates and thrust-drag evaluations. These curves have been included to show their relation to the other results.

Boattail pressure drag.- Examples of the experimental pressure distributions over the boattail from which boattail pressure-drag coefficients were obtained are shown in figure 4 for the sonic nozzle and in figure 5 for the supersonic nozzle. All of these results are for $M = 1.62$. In general, the effects of the primary jet and secondary flow were greatest at this Mach number and the indicated point of flow separation was farthest forward on the boattail. The effect of increasing $\frac{p_j}{p_\infty}$ and mass flow ratio w are in most instances similar to those obtained in reference 11 for the zero-length ejector, namely a general positive increase in the magnitude of the pressures and an increase in extent of the region affected. However, for some conditions increasing w from 0.10 to 0.20 had a negligible or slightly reverse effect $\Big($for example, see fig. 4, $\frac{p_j}{p_\infty} = 4.05$ and fig. 5, $\frac{p_j}{p_\infty} = 0.81\Big)$.

The boattail pressure-drag coefficient C_{D_A} was obtained as the sum of the graphical integration of the measured pressures from $\frac{x}{L} = 0.87$ to $\frac{x}{L} = 1$ plus the theoretical drag from the beginning of the boattail $\Big(\frac{x}{L} = 0.82\Big)$ to $\frac{x}{L} = 0.87$. With regard to the latter, the results of reference 11 showed that the theoretical pressures over the boattail were in good agreement with the experimental pressures ahead of the point of flow separation. In addition, the theoretical drag coefficient of the initial portion $\Big(\frac{x}{L} = 0.82$ to $0.87\Big)$ is small, ranging from about 0.0019 at $M = 1.62$ to 0.0013 at $M = 2.41$, and therefore represents a rather insignificant contribution to the boattail pressure drag. Consequently, moderate differences between the theoretical and experimental pressures over this initial portion would have negligible effect upon the value of C_{D_A}.

The variation of C_{D_A} with jet pressure ratio $\frac{p_j}{p_\infty}$ for the sonic nozzle is shown in figures 6(a) and 6(b) for diameter ratios of 1.50 and 1.33, respectively. With some exceptions in the lower range of $\frac{p_j}{p_\infty}$, the effects

of the addition of secondary flow for mass flow ratios up to 0.20 are, for wide ranges of primary jet operation, subordinate to the effects of the primary jet or varying $\frac{p_j}{p_\infty}$. For narrow ranges of primary jet operation $\left(\text{a change in } \frac{p_j}{p_\infty} \text{ of the order of } 4\right)$, the effects of $\frac{p_j}{p_\infty}$ and w may be comparable. As is to be expected, the variation of C_{D_A} with $\frac{p_j}{p_\infty}$ is of the same type as the variation of C_{D_B} with $\frac{p_j}{p_\infty}$; except at low values of $\frac{p_j}{p_\infty}$, increasing $\frac{p_j}{p_\infty}$ causes a decrease in C_{D_A} and this decrease is reduced by increasing Mach number. In all instances the addition of secondary flow as compared to the condition for $w = 0$ decreases C_{D_A}. For a fixed diameter ratio $\frac{d_s}{d_j}$ the magnitude of the drag reduction caused by a secondary flow and the effect of increasing mass flow ratio depend upon the particular combination of $\frac{p_j}{p_\infty}$, w, and M. In the lower range of $\frac{p_j}{p_\infty}$, increasing Mach number noticeably decreases the effect of increasing mass flow ratio. Aside from reducing this Mach number effect, decreasing the diameter ratio from 1.50 to 1.33 has only small effect (proper account being given to the values of C_{D_A} for jet off and no secondary flow, particularly at $M = 1.62$; see ref. 11).

Figure 7 presents the results for the supersonic nozzle. For narrow ranges of primary jet operation, these data show that the effects of mass flow ratio w may exceed the effects of jet pressure ratio $\frac{p_j}{p_\infty}$. This is particularly evident at $M = 1.62$. With increasing Mach number the effect of w is reduced. There are some effects of decreasing diameter ratio from 1.50 to 1.33, but with the exclusion of the results at $M = 1.62$ for $\frac{p_j}{p_\infty}$ near 1 and $w = 0.10$ to 0.20, these effects are small. When consideration is given to the difference in starting pressure ratios the major difference between the results for the sonic and supersonic nozzle appears to be that the effect of a small amount of secondary air flow is, at comparable values of $\frac{p_j}{p_\infty}$, generally greater for the supersonic nozzle.

Total afterbody drag.- The total afterbody drag is defined as the sum of the boattail pressure drag and the base drag. The results are shown in figures 8 and 9. Comparison of these results with the results presented in figures 2, 3, 6 and 7 shows that the total afterbody drag is determined primarily by the boattail pressure drag and that the observations given in the preceding section on boattail pressure drag also apply to the total afterbody drag.

Base drag would appear to contribute very little to the total afterbody drag for full-scale highly boattailed configurations since the ratio of the area of the base annulus to the maximum body frontal area for full-scale configurations is usually smaller than the ratios used in the present investigation. In comparison with the total drag of a complete configuration (wing-body-tail, and so forth) having an afterbody of this type, the power-on base drag and its variation with M, $\frac{p_j}{p_\infty}$, and w would be small indeed. The use of the area represented by $A_B - A_j$ in engineering estimates of the contribution of C_{D_B} to the total afterbody drag would appear generally conservative for $0 \leqq w \leqq 0.20$, notable exceptions occurring at $M = 1.62$ for the sonic nozzle at high jet pressure ratios. The present results suggest that equally and perhaps more satisfactory estimates of total afterbody drag for afterbodies of this type having comparable mass flow ratios could be made by assuming that C_{D_B} is zero.

Pumping Characteristics

The pumping characteristics will be presented as the total pressure ratio of the secondary air $\frac{p_{O_S}}{p_\infty}$ that is required to maintain a given mass-flow ratio w as the jet static-pressure ratio $\frac{p_j}{p_\infty}$ is varied. These results also show, of course, the effect of $\frac{p_j}{p_\infty}$ upon w at constant $\frac{p_{O_S}}{p_\infty}$.

Effect of diameter ratio.- The effect of decreasing the diameter ratio $\frac{d_s}{d_j}$ from 1.50 to 1.33 is shown in figure 10 for the sonic nozzle and in figure 11 for the supersonic nozzle. In fairing the curves for

$w = 0$ what appears to be a cut-off value of $\dfrac{p_j}{p_\infty}$ could not be sharply

defined by the customary abrupt change in slope because of insufficient data points. The fairing of the curves for $w = 0$ is, therefore, questionable in these regions. $\left(\text{See fig. 10(a), for example, } \dfrac{p_j}{p_\infty} = 8 \text{ to } 16\right.$

for $\dfrac{d_s}{d_j} = 1.50.$ $\Big)$ From simple continuity considerations, the effect of

decreasing $\dfrac{d_s}{d_j}$ would be expected to be significant and in the direction

indicated by the experimental results, namely, an increase in $\dfrac{p_{O_s}}{p_\infty}$ for

constant $\dfrac{p_j}{p_\infty}$ and w.

Effect of free-stream Mach numbers.- The question of the possible effects of free-stream Mach number upon pumping characteristics and the applicability of results from studies of ejectors exhausting into still air may be resolved to some degree by a few simple considerations. If the value of $\dfrac{p_j}{p_\infty}$ is moderately greater than that for which the primary

jet first fills the ejector and results in the combined primary and secondary flow being well supersonic throughout at the ejector exit, changes in free stream Mach number cannot be expected to affect the pumping characteristics other than through negligible effects upon the ejector boundary layer near the ejector exit. Under these conditions changes in free-stream Mach number will only affect the degree of expansion, or compression, of the ejector flow at the ejector exit. (Of course $\dfrac{p_j}{p_\infty}$ under these assumed conditions is always greater than that

for separation of the supersonic ejector flow from the ejector wall by a compression at the ejector exit.) It becomes clear, therefore, that changes in base pressure do not necessarily mean changes in pumping characteristics. If, however, the value of $\dfrac{p_j}{p_\infty}$ is less than that for

the conditions just described, free-stream Mach number may affect the pumping characteristics. It is obvious that the pumping characteristics for a zero-length ejector will always be affected by base pressure which in turn is affected by free-stream Mach number; at $w = 0$ the value of $\dfrac{p_{O_s}}{p_\infty}$ for such an ejector is equal to $\dfrac{p_B}{p_\infty}$ at all values of $\dfrac{p_j}{p_\infty}$.

Consequently, it is appropriate to think of the possible effects of free-stream Mach number upon $\frac{p_{o_s}}{p_\infty}$ in terms of its effects upon $\frac{p_B}{p_\infty}$. From prior investigations of jet effects upon base pressure with varying free-stream Mach number, $\frac{p_B}{p_\infty}$ is observed to be of the order of 1 and usually less; the maximum effect of free-stream Mach number upon $\frac{p_{o_s}}{p_\infty}$ should therefore be of the same order.

Figure 12 presents examples of the pumping characteristics for the tests of the model of this investigation with zero-length ejector reported in reference 11. These results show that except at low mass-flow ratios and jet static-pressure ratios, free-stream Mach number has only secondary effects as compared to the effects of w and $\frac{p_j}{p_\infty}$. The values of $\frac{p_{o_s}}{p_\infty}$ at low w (less than about 0.02) and low $\frac{p_j}{p_\infty}$ are of the order of magnitude of $\frac{p_B}{p_\infty}$ and the maximum effect of free-stream Mach number is seen to be, in general, of this order. In view of these results for the zero-length ejector (spacing ratio of zero), a finite positive spacing ratio would be expected to show even less effect of free-stream Mach number, with the possible exception of very low values of $\frac{p_j}{p_\infty}$. This is confirmed by the by the present results (spacing ratio of 0.19) which are shown in figures 13 and 14. On the basis of these results and those of figure 12, and in view of the fact that these data are for configurations which would be prone to accentuate effects of free stream Mach number, it would appear permissible to conclude that ejectors most likely to be encountered in full-scale installations will experience little effect of free-stream Mach number upon their pumping characteristics. The results of reference 10 for a diameter ratio of 1.2 and a spacing ratio of 0.8 show no effect of free-stream Mach number.

The present results (figs. 13 and 14) show that the value of $\frac{p_j}{p_\infty}$ at which free-stream Mach number ceases to affect the pumping characteristics tends to decrease with increasing mass-flow ratio. In figure 13(b) a dashed curve is shown for $w = 0.10$ which was derived through interpolations and extrapolations to the results of reference 21 for ejectors

exhausting into still air. The tendency toward agreement with the present results is encouraging from the standpoint of the applicability of results from ejector tests in still air. For the larger spacing ratio of reference 10, good agreement was shown with the results of reference 21 when proper account was given to the vena contracta effect common to the configuration of reference 10.

Effect of spacing ratio.- A comparison of figure 12 with figures 13 and 14 reveals that changing the spacing ratio from zero to 0.19 had only small effects upon the pumping characteristics for the supersonic nozzle. At comparable values of $\frac{p_j}{p_\infty}$ (less than about 8) the same was true for the sonic nozzle. However, at the higher values of $\frac{p_j}{p_\infty}$ reached with the sonic nozzle only, the values of $\frac{p_{o_s}}{p_\infty}$ at $w = 0.02$ and at both diameter ratios were generally greater for a spacing ratio of 0.19, and this difference tended to increase with $\frac{p_j}{p_\infty}$; at $w = 0.10$ the same general effect occurred at $\frac{d_j}{d_s} = 1.50$, but at $\frac{d_j}{d_s} = 1.33$ the effect of this change in spacing ratio was minor.

Effect of type of primary nozzle.- A comparison of the results for the sonic nozzle (fig. 13) with those for the supersonic nozzle (fig. 14) shows that only at low values of w and $\frac{p_j}{p_\infty}$ do these nozzles have similar pumping characteristics. At higher values the supersonic nozzle requires several times the value of $\frac{p_{o_s}}{p_\infty}$ required by the sonic nozzle at equivalent values of w and $\frac{p_j}{p_\infty}$. This is also true for the zero-length ejector, and, referring to the preceding paragraph, one may conclude that this difference between the sonic and supersonic nozzles is not significantly associated with flow conditions within the jector but is determined primarily by conditions at or downstream of the ejector exit. From a consideration of only the viscous scavenging effects of the jet upon the secondary air, one might expect a decrease in $\frac{p_{o_s}}{p_\infty}$ for the supersonic nozzle. However, if the combined effects of jet Mach number and nozzle

geometry (divergence angle of 12° in particular) upon the shape of the initial portion of the free jet boundary as shown in reference 23 are also considered, the increase in $\dfrac{p_{O_S}}{p_{\infty}}$ for the supersonic nozzle is not too surprising.

Schlieren observations.- Figure 15 presents a typical schlieren photograph illustrating the basic features of the observed flow and model installations at $M = 1.62$, and figure 16 presents a few sequences obtained at the same Mach number which illustrate the effects of $\dfrac{p_j}{p_{\infty}}$, w, and $\dfrac{d_s}{d_j}$. Comparison of figures 16(a) and 16(b) would tentatively indicate that some of the increase in $\dfrac{p_{O_S}}{p_{\infty}}$ associated with decreasing $\dfrac{d_s}{d_j}$ might, at the higher mass-flow ratios, be attributable to the earlier appearance of shocks within the jet other than those associated with normal jet structure (see ref. 23), for example, at $w = 0.20$ and $\dfrac{p_j}{p_{\infty}} = 0.81$. Comparison of figures 16(b) and 16(c) might lead one to suspect that a major cause of the higher values of $\dfrac{p_{O_S}}{p_{\infty}}$ for the supersonic nozzle, as compared to the sonic nozzle, is the presence and strength of the additional shocks for the supersonic nozzle; for example, at $w = 0.20$ the supersonic nozzle shows that a strong additional shock is already present at $\dfrac{p_j}{p_{\infty}} = 0.81$, whereas the sonic nozzle may operate at least to $\dfrac{p_j}{p_{\infty}} = 2.02$ with practically no abnormal change in jet structure. These phenomena might be taken to suggest that the supersonic nozzle, by induction effects and geometry, succeeds in choking the ejector at lower values of $\dfrac{p_j}{p_{\infty}}$ and that the additional shocks are required by the turning of the supersonic flow by the shroud surface; the pressure-rise through shocks thus generated would increase $\dfrac{p_{O_S}}{p_{\infty}}$. However, such an explanation for the increase in $\dfrac{p_{O_S}}{p_{\infty}}$ must be invalid, since a similar increase has already been shown to occur for the case of the zero-length ejector. These additional shocks, therefore, cannot be considered the cause of the large differences between the sonic and supersonic nozzle or to contribute significantly to the

increase in $\dfrac{p_{o_s}}{p_\infty}$ with decreasing $\dfrac{d_s}{d_j}$. They may play a more important

role in the variation of $\dfrac{p_{o_s}}{p_\infty}$ with w, but this too appears doubtful,

notwithstanding the effect that increasing w is observed to have in increasing the strength of existing shocks or in creating additional

shocks. Indications are that at some combinations of low $\dfrac{p_j}{p_\infty}$ and

high w the secondary flow will choke the secondary annulus in the plane of the primary nozzle exit. Under these conditions the presence of additional shocks is a logical expectation.

General Remarks

The application of the results which have been presented herein should be confined to configurations resembling closely those employed in this investigation. Particular care should be exercised in applying the pumping characteristics. In reference 10, the geometry of the secondary passage was shown to be important to the pumping characteristics; in this investigation nozzle geometry is indicated to be of importance. The possible effects of these variables, coupled with the effects of spacing ratio and diameter ratio, deserve special attention.

CONCLUSIONS

An investigation has been conducted to determine the external drag effects and pumping characteristics of a short ejector having a spacing ratio of 0.19 and housed within a highly boattailed afterbody. Tests were made at free-stream Mach numbers of 1.62, 1.94, and 2.41 for secondary to primary diameter ratios, 1.50 and 1.33, and for a sonic and supersonic primary nozzle. Mass-flow ratio was varied from 0 to 0.20. The following conclusions are indicated:

1. The contribution of the base drag to the total afterbody drag was small at all mass-flow ratios and jet static-pressure ratios, with minor exceptions at low jet static-pressure ratios. The effect of the primary jet and secondary flow upon boattail pressure drag was the predominant factor in determining the effects upon total afterbody drag.

2. The variation of base drag, boattail pressure drag, and total afterbody drag exhibited conventional effects from increasing jet static-pressure ratio, namely, a decrease with increasing jet static-pressure ratio except at low jet static-pressure ratios where the converse was true. The addition of secondary flow caused a decrease in

these drags and, with few exceptions, the reductions in drag tended to increase with increasing mass flow ratio.

3. In general, increasing free-stream Mach number reduced the effects of mass-flow ratio and jet static-pressure ratio upon the drag.

4. When consideration is given to the difference in the jet static-pressure ratios for starting, the drag results for the supersonic nozzle and sonic nozzle were similar. The only major difference was the tendency of a small amount of secondary air flow to have, in general, a greater effect with the supersonic nozzle.

5. A cursory comparison of the results of this investigation with the results of NACA RM L54I22 (same model employed in this investigation but with a zero-length ejector) indicated that changing the spacing ratio from 0 to 0.19 did not significantly alter the effects of the primary jet or secondary flow upon the drag.

6. In general, decreasing the diameter ratio from 1.50 to 1.33 had only small effect upon the drag but, of course, had significant effect upon the pumping characteristics, which were conventional insofar as the effects of jet static-pressure ratio, mass-flow ratio, and diameter ratio were concerned.

7. The effect of free-stream Mach number upon the pumping characteristics was negligible except at low jet static-pressure ratios where the effect was generally small. The present results and a comparison with results from the investigation of NACA RM L54I22 for the zero-length ejector tend to indicate that when free-stream Mach number does affect the pumping characteristics of an ejector, these effects will most likely be small.

8. A comparison with the results for the zero-length ejector indicated that changing the spacing ratio from 0 to 0.19 had only small effect on the pumping characteristics for the supersonic nozzle and for the sonic nozzle at comparable jet static-pressure ratios (up to about 8). At the higher jet static-pressure ratios reached with the sonic nozzle only, the pumping characteristics were, in some instances, significantly affected by this change in spacing ratio.

9. The pumping characteristics of the sonic and supersonic nozzle were notably different. The geometry and exit Mach number of a supersonic primary nozzle appear to be important in determining the pumping characteristics.

Langley Aeronautical Laboratory,
    National Advisory Committee for Aeronautics,
        Langley Field, Va., April 12, 1955.

REFERENCES

1. Love, Eugene S.: Aerodynamic Investigation of a Parabolic Body of
     Revolution at Mach Number of 1.92 and Some Effects of an Annular
     Jet Exhausting From the Base. NACA RM L9K09, 1950.

2. Stoney, William E., Jr., and Katz, Ellis: Pressure Measurements on
     a Sharply Converging Fuselage Afterbody With Jet On and Off at Mach
     Numbers From 0.8 to 1.6. NACA RM L50F06, 1950.

3. Purser, Paul E., Thibodaux, Joseph G., and Jackson, H. Herbert: Note
     on Some Observed Effects of Rocket-Motor Operation on the Base Pres-
     sure of Bodies in Free Flight. NACA RM L50I18, 1950.

4. Cortright, Edgar M., Jr., and Schroeder, Albert H.: Investigation at
     Mach Number 1.91 of Side and Base Pressure Distributions Over Coni-
     cal Boattails Without and With Jet Flow Issuing From Base. NACA
     RM E51F26, 1951.

5. Gillespie, Warren, Jr.: Jet Effects on Pressures and Drags of Bodies.
     NACA RM L51J29, 1951.

6. Cantrell, H. N., and Gazley, Carl, Jr.: Base Pressure on Bodies of
     Revolution at Subsonic and Supersonic Velocities With and Without
     Jet Exhausts. PROJECT HERMES Aero. Fundamentals Memo. #18, Gen.
     Elec. Co., Apr. 11, 1952.

7. Cortright, Edgar M., Jr., and Kochendorfer, Fred D.: Jet Effects on
     Flow Over Afterbodies in Supersonic Stream. NACA RM E53H25, 1953.

8. Englert, Gerald W., Vargo, Donald J., and Cubbison, Robert W.: Effect
     of Jet-Nozzle-Expansion Ratio on Drag of Parabolic Afterbodies.
     NACA RM E54B12, 1954.

9. De Moraes, Carlos A., and Nowitzky, Ablin M.: Experimental Effects of
     Propulsive Jets and Afterbody Configurations on the Zero-Lift Drag
     of Bodies of Revolution at a Mach Number of 1.59. NACA RM L54C16,
     1954.

10. Gorton, Gerald C.: Pumping and Drag Characteristics of an Aircraft
     Ejector at Subsonic and Supersonic Speeds. NACA RM E54D06, 1954.

11. O'Donnell, Robert M., and McDearmon, Russell W.: Experimental Inves-
     tigation of Effects of Primary Jet Flow and Secondary Flow Through
     a Zero-Length Ejector on Base and Boattail Pressures of a Body of
     Revolution at Free-Stream Mach Numbers of 1.62, 1.93, and 2.41.
     NACA RM L54I22, 1954.

12. Bromm, August F., Jr., and O'Donnell, Robert M.: Investigation at
    Supersonic Speeds of the Effect of Jet Mach Number and Divergence
    Angle of the Nozzle Upon the Pressure on the Base Annulus of a
    Body of Revolution. NACA RM L54I16, 1954.

13. Hearth, Donald P., and Gorton, Gerald C.: Investigation of Thrust and
    Drag Characteristics of a Plug-Type Exhaust Nozzle. NACA RM E53L16,
    1954.

14. Vargo, Donald J., and Englert, Gerald W.: Effect of Nozzle Contour on
    Drag of Parabolic Afterbodies. NACA RM E54D02, 1954.

15. Hearth, Donald P., and Wilcox, Fred A.: Thrust and Drag Characteris-
    tics of a Convergent-Divergent Nozzle With Various Exhaust Jet Tem-
    peratures. NACA RM E53L23b, 1954.

16. Greathouse, W. K., and Hollister, D. P.: Preliminary Air-Flow and
    Thrust Calibrations of Several Conical Cooling-Air Ejectors With
    a Primary to Secondary Temperature Ratio of 1.0. I - Diameter
    Ratios of 1.21 and 1.10. NACA RM E52E21, 1952.

17. Greathouse, W. K. and Hollister, D. P.: Preliminary Air Flow and
    Thrust Calibrations of Several Conical Cooling-Air Ejectors With
    a Primary to Secondary Temperature Ratio of 1.0. II - Diameter
    Ratios of 1.06 and 1.40. NACA RM E52F26, 1952.

18. Ellis, C. W., Hollister, D. P., and Wilsted, H. D.: Investigation
    of Performance of Several Double-Shroud Ejector and Effect of
    Variable-Area Exhaust Nozzle on Single Ejector Performance. NACA
    RM E52D25, 1952.

19. Reshotko, Eli: Performance Characteristics of a Double-Cylindrical-
    Shroud Ejector Nozzle. NACA RM E53H28, 1953.

20. Hollister, Donald P., and Greathouse, William K.: Performance of
    Double-Shroud Ejector Configuration With Primary Pressure Ratios
    From 1.0 to 10. NACA RM E52K17, 1953.

21. Greathouse, W. K., and Hollister, D. P.: Air-Flow and Thrust Charac-
    teristics of Several Cylindrical Cooling-Air Ejectors With a Pri-
    mary to Secondary Temperature Ratio of 1.0. NACA RM E52L25, 1953.

22. Huntley, S. C., and Yanowitz, Herbert: Pumping and Thrust Charac-
    teristics of Several Divergent Cooling-Air Ejectors and Comparison
    of Performance With Conical and Cylindrical Ejectors. NACA
    RM E53J13, 1954.

23. Love, Eugene S., and Grigsby, Carl E.: Some Studies of Axisymmetric
    Free Jets Exhausting From Sonic and Supersonic Nozzles Into Still
    Air and Into Supersonic Streams. NACA RM L54L31, 1955.

Primary flow

Primary pressure conduits

Primary stagnation chamber

Support strut for supersonic nozzle

Sonic nozzle

1.53

8.25

$3\frac{11}{16}$

1.25

1.50

Transition strip

d_s d_B

$\frac{1}{8}$ $\frac{13}{16}$ $\frac{5}{8}$ 0.071

$\frac{7}{16}$

Secondary total-pressure tube

Secondary pressure conduits

Instrumentation channel

Base annulus

Secondary flow

Rear view of base-pressure orifices

Base characteristics

Shroud	d_s	d_B	d_s/d_B	A_N/A_{max}
1	9/16	11/16	0.82	0.100
2	1/2	11/16	0.73	0.1425

$2\frac{9}{16}$

$12°$

$\frac{3}{8}$

Supersonic nozzle (M=3.23)

1 2 3 4 5

4.140^R

Z

Orifice positions

Orifice	Z
1	1.06
2	0.79
3	0.53
4	0.29
5	0.06

Figure 1.- Sketch of model and wing supports. All dimensions are in inches.

(a) First shroud $\left(\dfrac{d_s}{d_j} = 1.50\right)$.
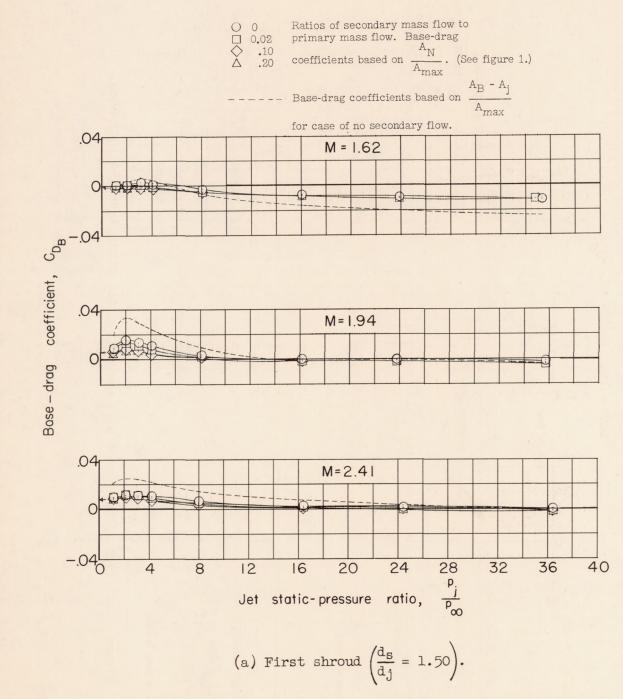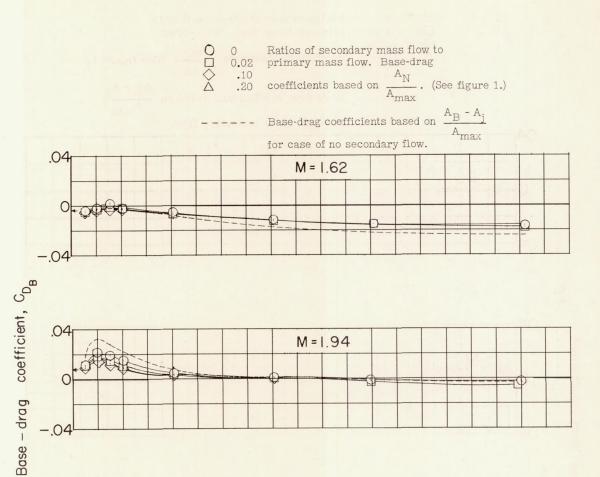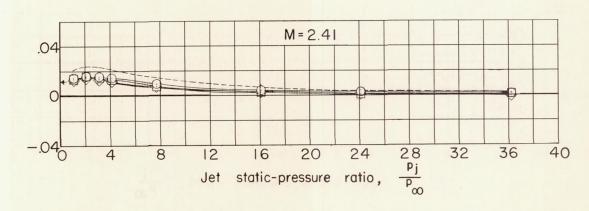
Figure 2.- Variation of base-drag coefficient with jet-static pressure ratio, mass-flow ratio, and free-stream Mach number. Sonic nozzle.

○   0   Ratios of secondary mass flow to
□   0.02   primary mass flow. Base-drag
◇   .10   coefficients based on $\dfrac{A_N}{A_{max}}$. (See figure 1.)
△   .20

- - - - - -   Base-drag coefficients based on $\dfrac{A_B - A_j}{A_{max}}$

for case of no secondary flow.
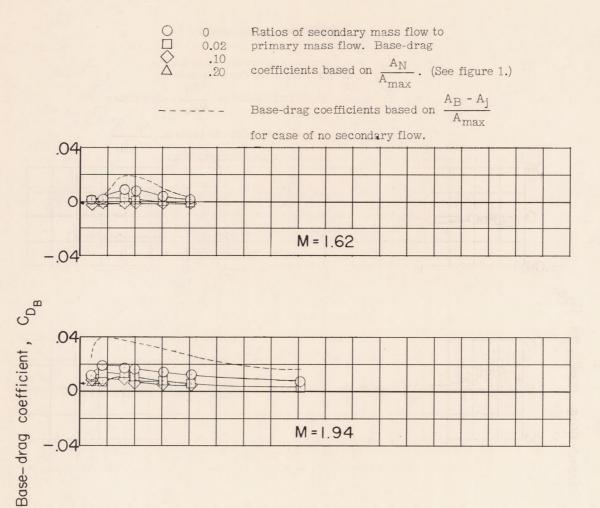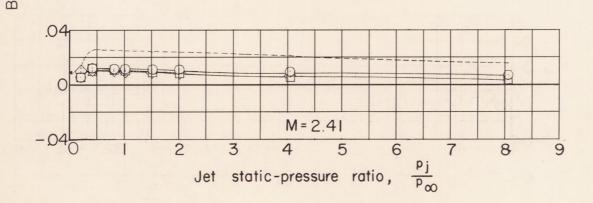
(b) Second shroud $\left(\dfrac{d_s}{d_j} = 1.33\right)$.

Figure 2.- Concluded.

○　　0　　　Ratios of secondary mass flow to
□　　0.02　　primary mass flow. Base-drag
◇　　.10
△　　.20　　coefficients based on $\dfrac{A_N}{A_{max}}$. (See figure 1.)

------　Base-drag coefficients based on $\dfrac{A_B - A_j}{A_{max}}$

for case of no secondary flow.

M = 1.62

M = 1.94

M = 2.41

Base-drag coefficient, C_{D_B}

Jet static-pressure ratio, $\dfrac{p_j}{p_\infty}$

(a) First shroud $\left(\dfrac{d_s}{d_j} = 1.50\right)$.
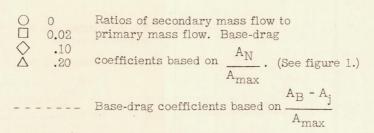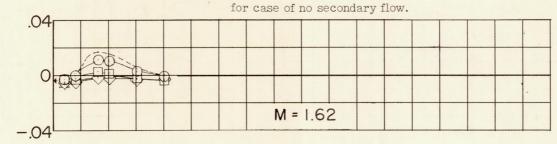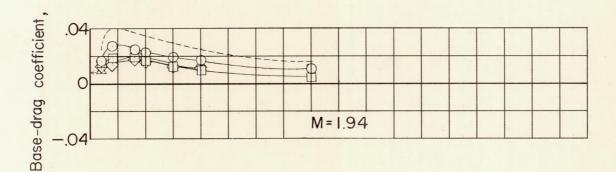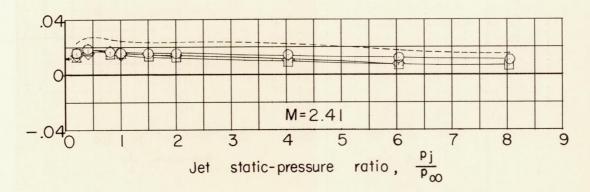
Figure 3.- Variation of base-drag coefficient with jet-static pressure
ratio, mass-flow ratio, and free-stream Mach number. Supersonic
nozzle.

○   0   Ratios of secondary mass flow to
□   0.02   primary mass flow. Base-drag
◇   .10   coefficients based on $\dfrac{A_N}{A_{max}}$. (See figure 1.)
△   .20

------- Base-drag coefficients based on $\dfrac{A_B - A_j}{A_{max}}$

for case of no secondary flow.

$M = 1.62$

$M = 1.94$

$M = 2.41$

Jet static-pressure ratio, $\dfrac{p_j}{p_\infty}$
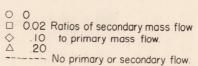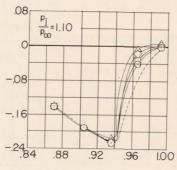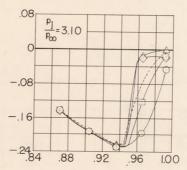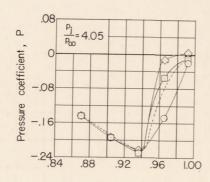
(b) Second shroud $\left(\dfrac{d_s}{d_j} = 1.33\right)$.
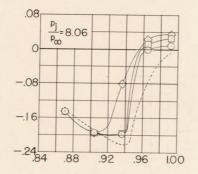
Figure 3.- Concluded.
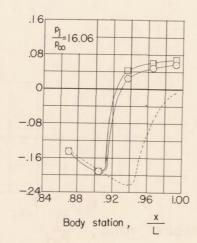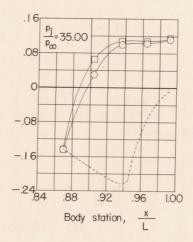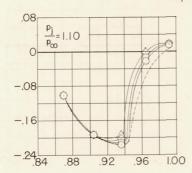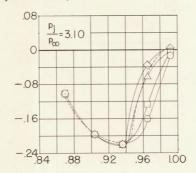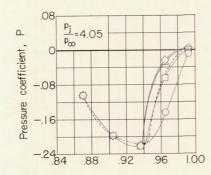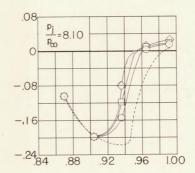
(a) First shroud $\left(\dfrac{d_s}{d_j} = 1.50\right)$.
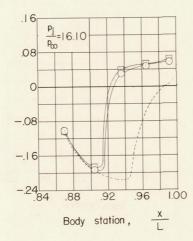
Figure 4.- Examples of pressure distribution over boattail surface at
M = 1.62.   Sonic nozzle.

○   0
□   0.02 Ratios of secondary mass flow
◇   .10   to primary mass flow.
△   .20
------ No primary or secondary flow.
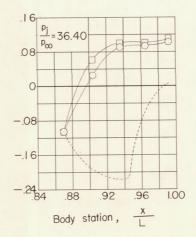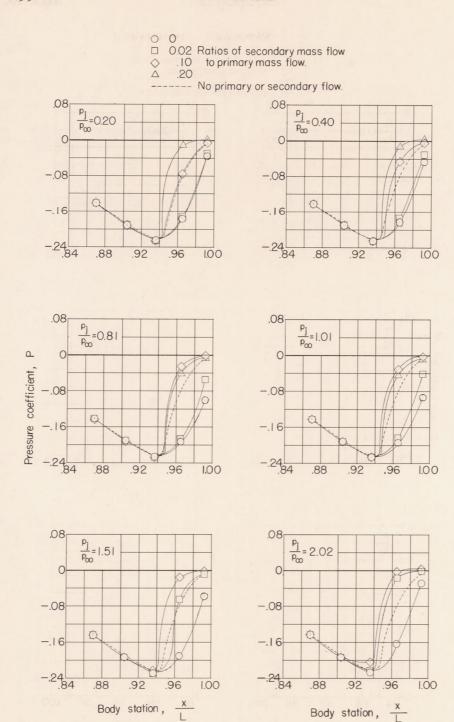
(b) Second shroud $\left(\dfrac{d_s}{d_j} = 1.33\right)$.

Figure 4.- Concluded.

CONFIDENTIAL
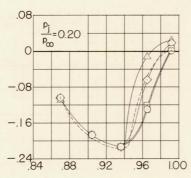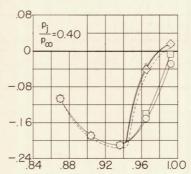
(a) First shroud $\left(\dfrac{d_S}{d_j} = 1.50\right)$.
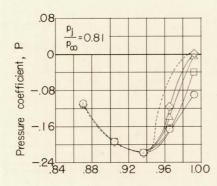
Figure 5.- Examples of pressure distribution over boattail surface at M = 1.62. Supersonic nozzle.
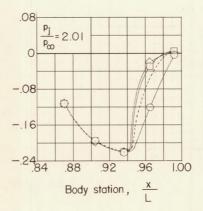
(b) Second shroud $\left(\dfrac{d_s}{d_j} = 1.33\right)$.

Figure 5.- Concluded.

(a) First shroud $\left(\dfrac{d_s}{d_j} = 1.50\right)$.
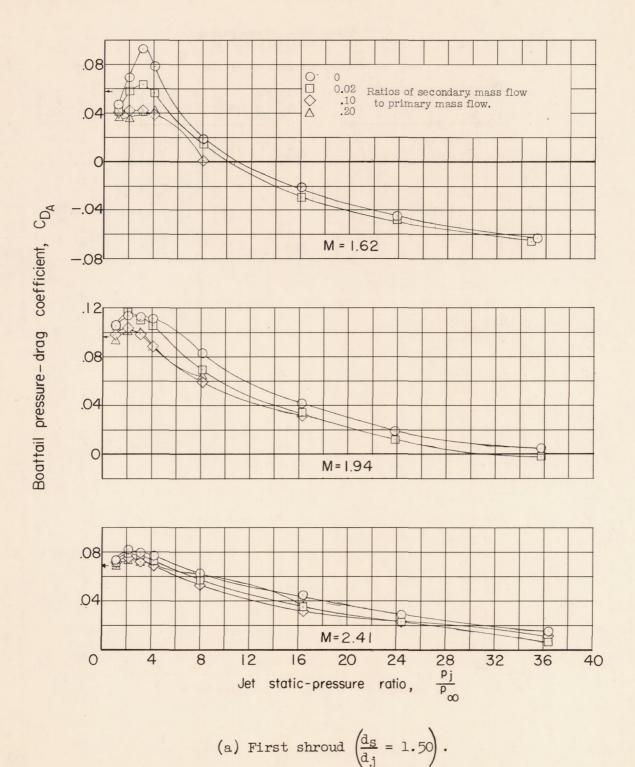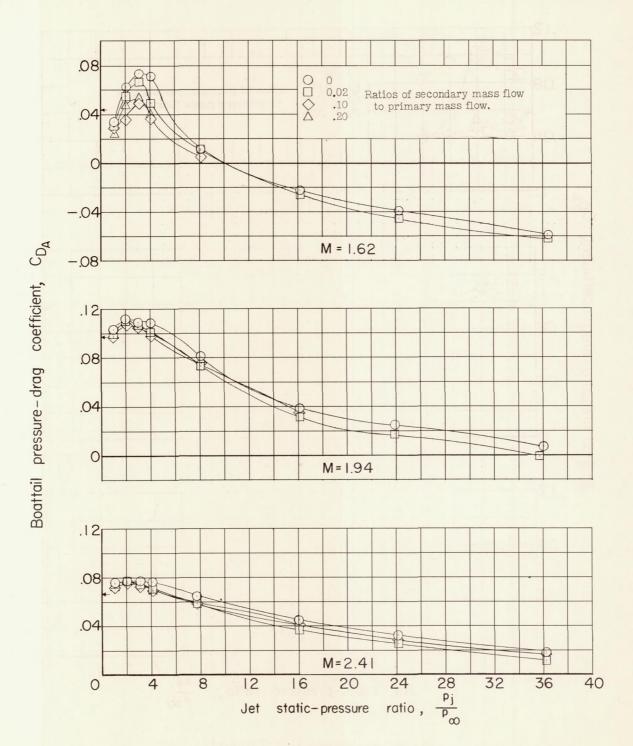
Figure 6.- Variation of boattail pressure-drag coefficient with jet-
     static pressure ratio, mass-flow ratio, and free-stream Mach number.
     Sonic nozzle.

(b) Second shroud $\left(\dfrac{d_s}{d_j} = 1.33\right)$.

Figure 6.- Concluded.

(a) First shroud $\left(\dfrac{d_s}{d_j} = 1.50\right)$.
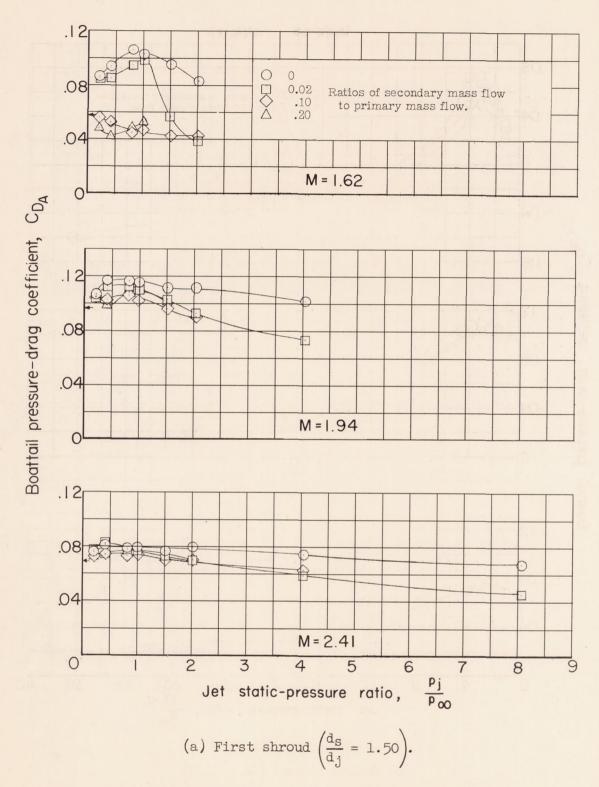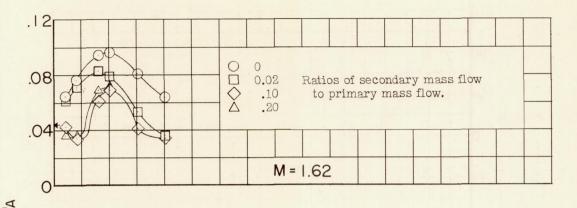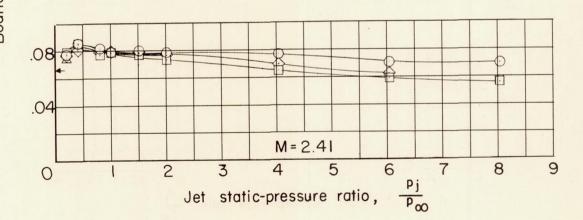
Figure 7.- Variation of boattail pressure-drag coefficient with jet-static pressure ratio, mass-flow ratio, and free-stream Mach number. Supersonic nozzle.

(b) Second shroud $\left(\dfrac{d_s}{d_j} = 1.33\right)$.

Figure 7.- Concluded.

(a) First shroud $\left(\dfrac{d_s}{d_j} = 1.50\right)$.
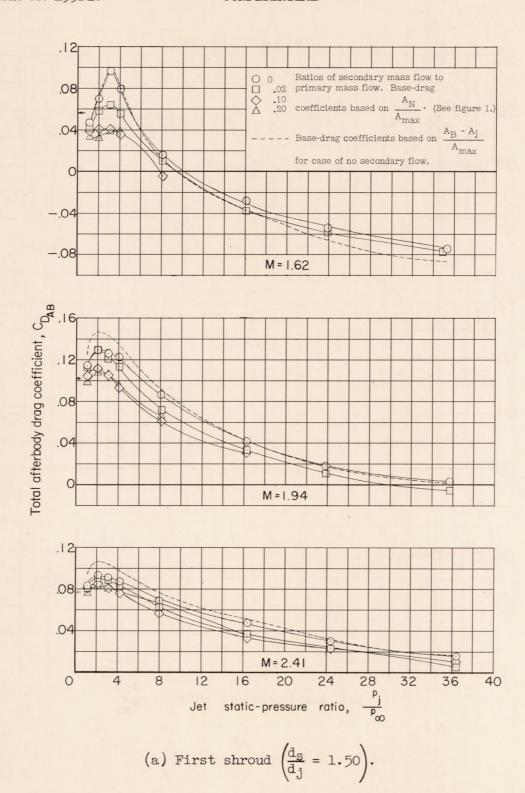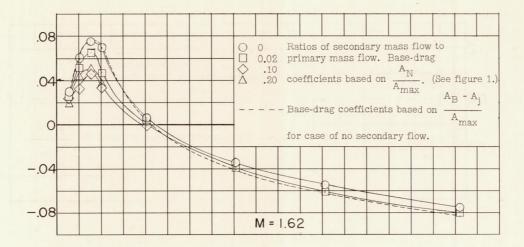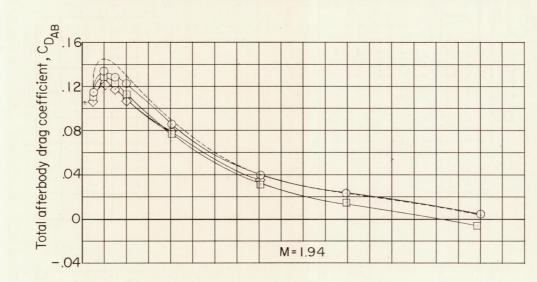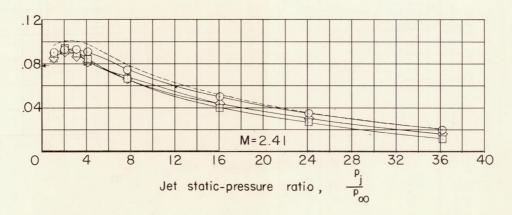
Figure 8.- Variation of total afterbody drag coefficient with jet-static pressure ratio, mass-flow ratio, and free-stream Mach number. Sonic nozzle.
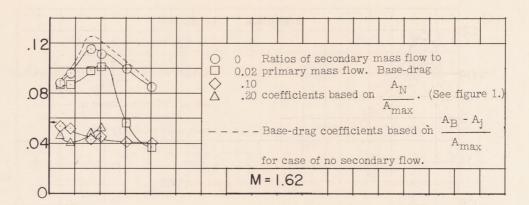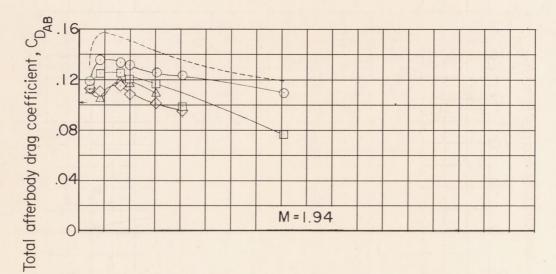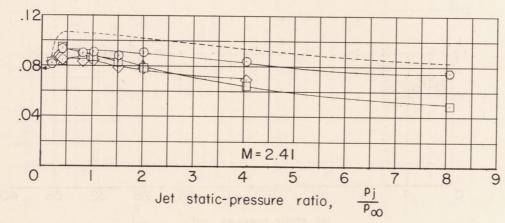
(b) Second shroud $\left(\dfrac{d_s}{d_j} = 1.33\right)$.

Figure 8.- Concluded.
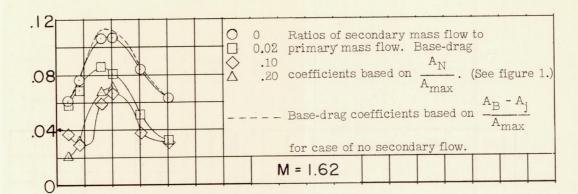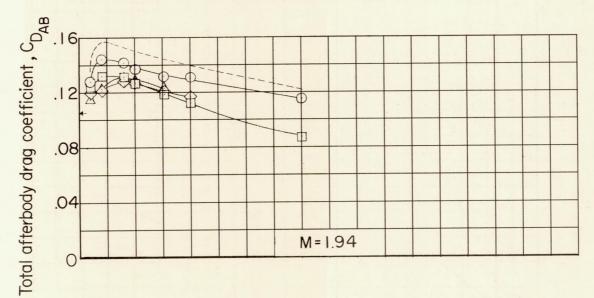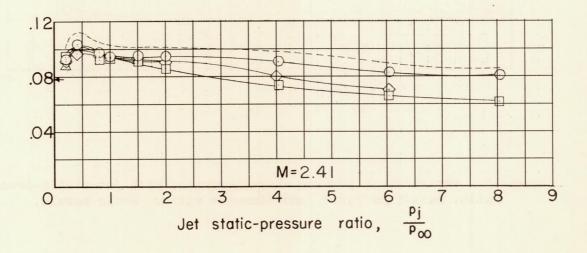
(a) First shroud $\left(\dfrac{d_s}{d_j} = 1.50\right)$.

Figure 9.- Variation of total afterbody drag coefficient with jet-static
    pressure ratio, mass-flow ratio, and free-stream Mach number. Super-
    sonic nozzle.

The legend in the figure reads:

○ 0   Ratios of secondary mass flow to

□ 0.02 primary mass flow. Base-drag

◇ .10   coefficients based on $\dfrac{A_N}{A_{max}}$. (See figure 1.)

△ .20

- - - - - Base-drag coefficients based on $\dfrac{A_B - A_j}{A_{max}}$

for case of no secondary flow.

M = 1.62

M = 1.94

M = 2.41

Total afterbody drag coefficient, $C_{D_{AB}}$

Jet static-pressure ratio, $\dfrac{p_j}{p_\infty}$

(b) Second shroud $\left(\dfrac{d_s}{d_j} = 1.33\right)$.

Figure 9.- Concluded.

(a) M = 1.62.
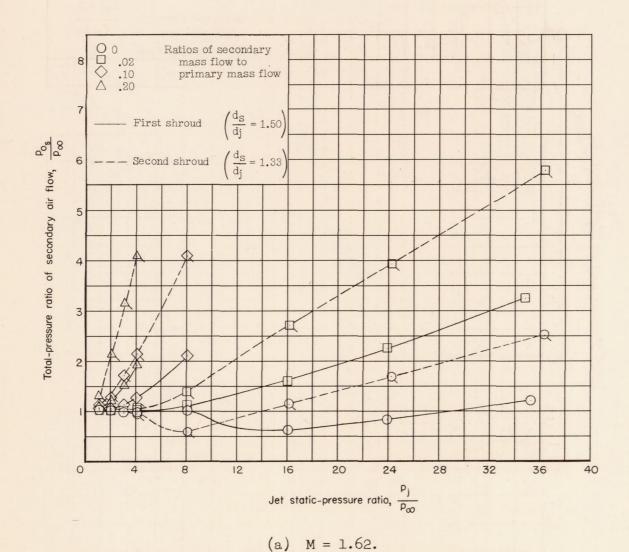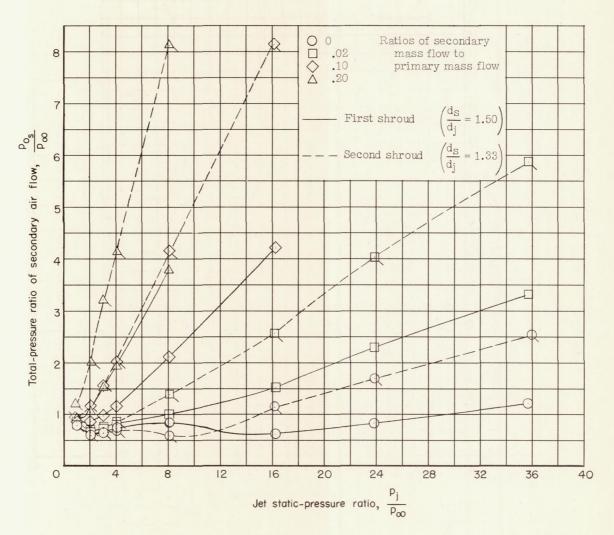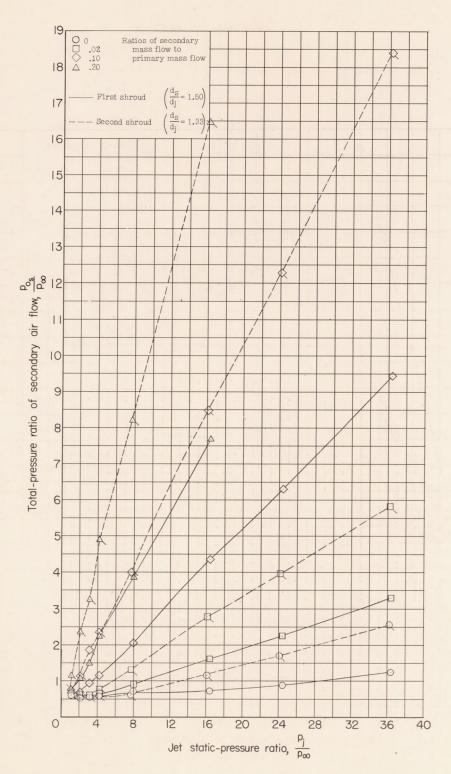
Figure 10.- Variation of pumping characteristics with jet static-pressure ratio, mass-flow ratio, and diameter ratio. Sonic nozzle.

(b) M = 1.94.

Figure 10.- Continued.

(c) M = 2.41.

Figure 10.- Concluded.

(a) M = 1.62.

(b) M = 1.94.
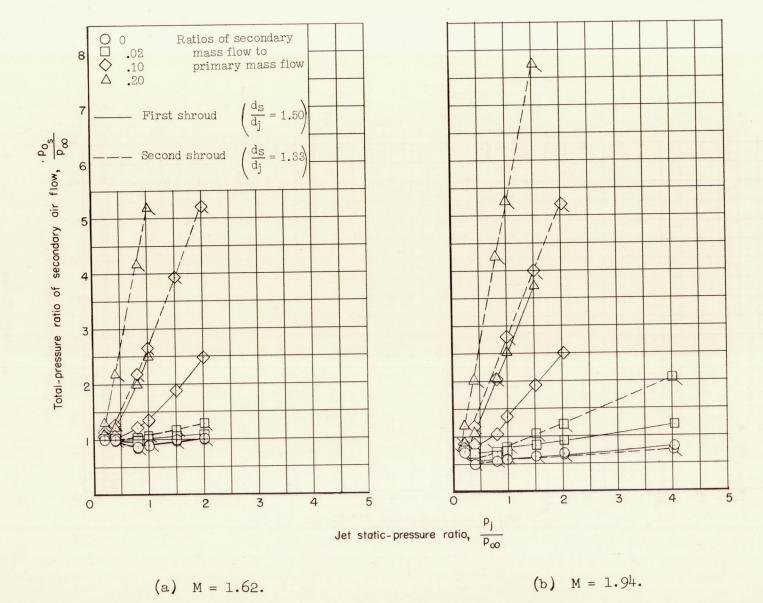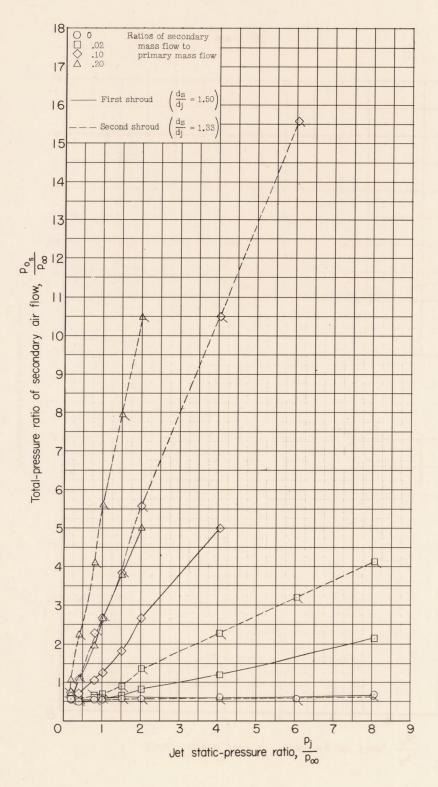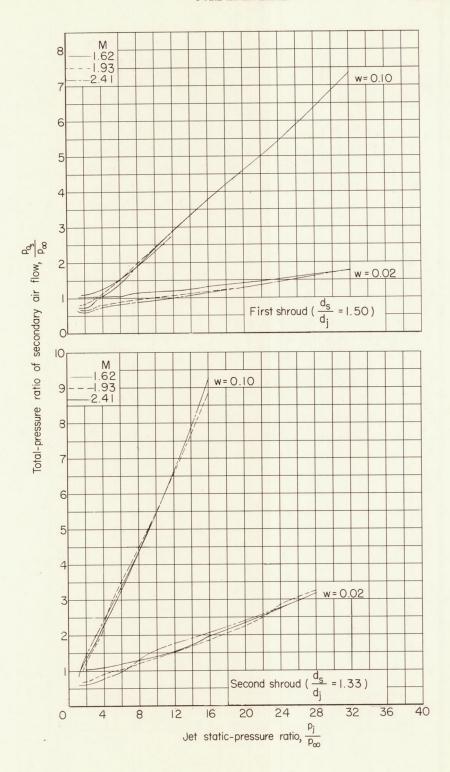
Figure 11.- Variation of pumping characteristics with jet-static pressure
ratio, mass-flow ratio, and diameter ratio. Supersonic nozzle.
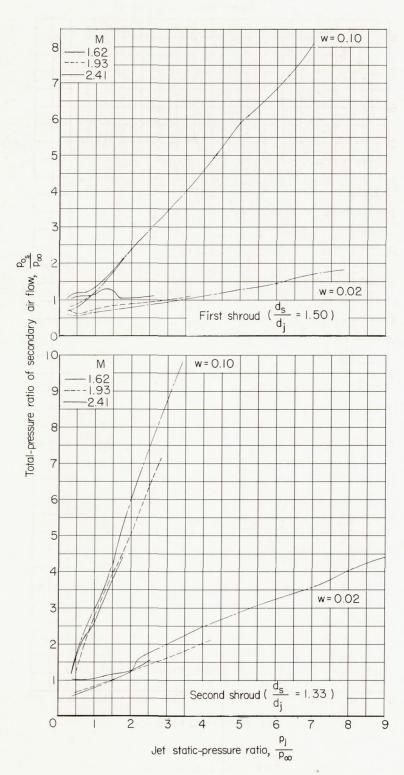
(c) M = 2.41.

Figure 11.- Concluded.
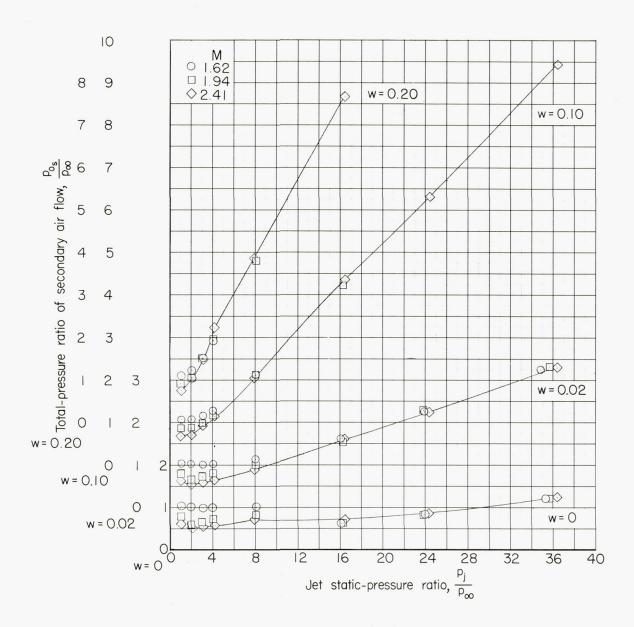
(a) Sonic nozzle.

Figure 12.- Pumping characteristics of model of this investigation with a zero-length ejector. Data obtained in investigation of reference 11.
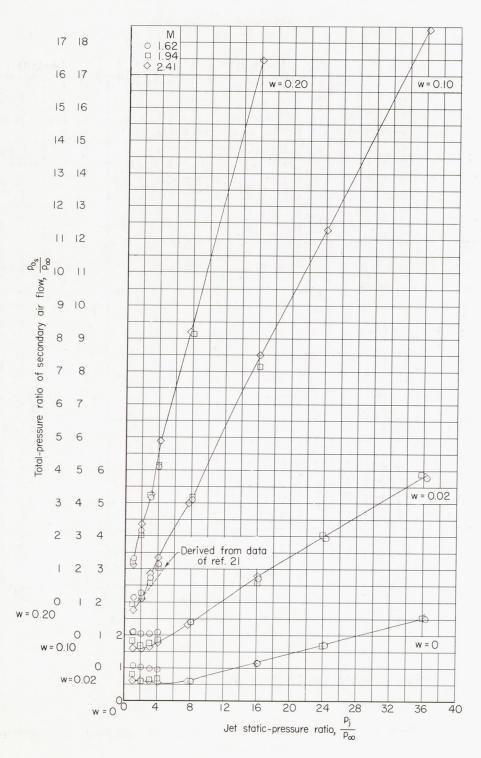
(b) Supersonic nozzle.

Figure 12.- Concluded.
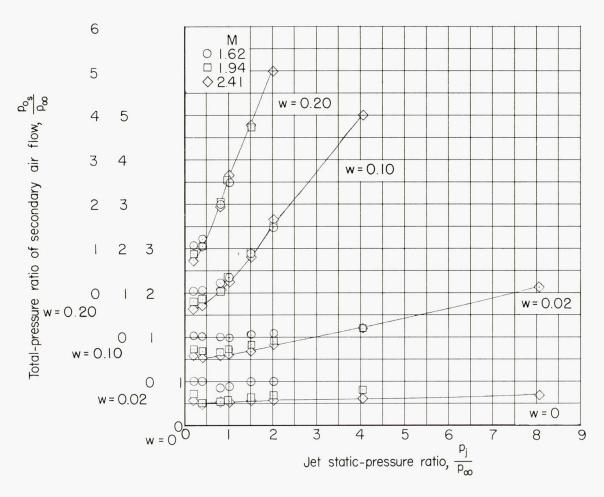
(a) First shroud $\left(\dfrac{d_s}{d_j} = 1.50\right)$.

Figure 13.- Effect of free-stream Mach number on pumping characteristics. Sonic nozzle.
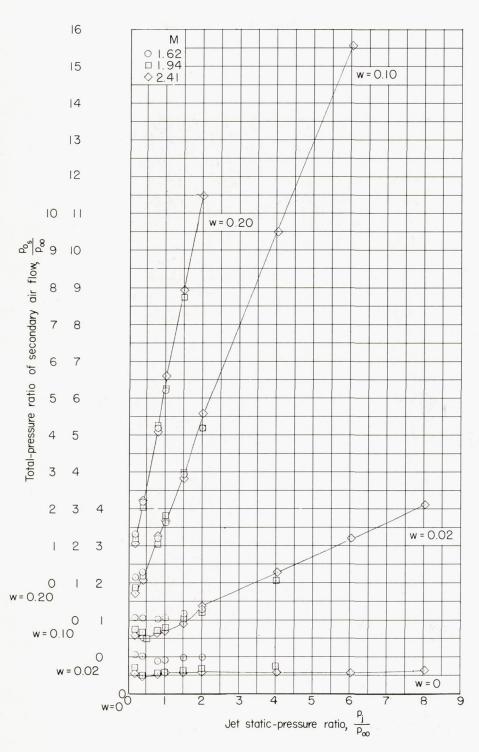
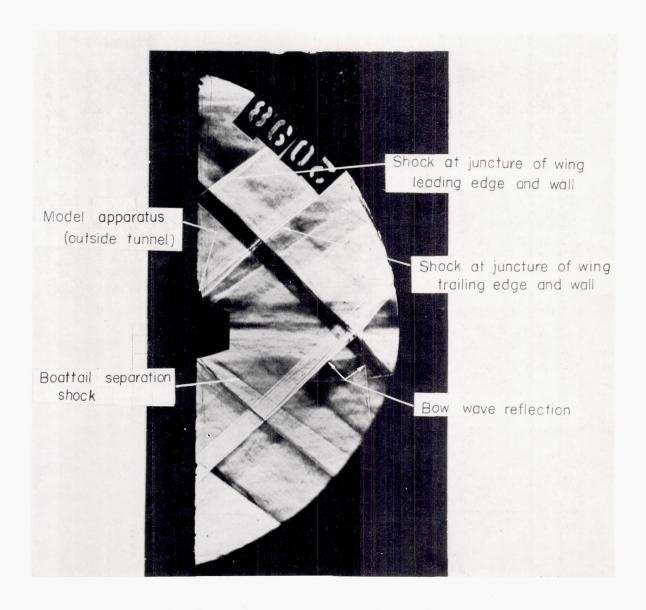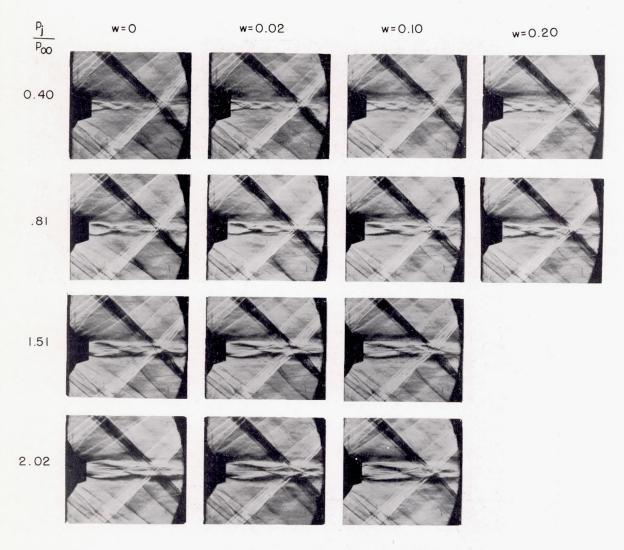(b) Second shroud $\left(\dfrac{d_s}{d_j} = 1.33\right)$.

Figure 13.- Concluded.

(a) First shroud $\left(\dfrac{d_s}{d_j} = 1.50\right)$.

Figure 14.- Effect of free-stream Mach number on pumping characteristics. Supersonic nozzle.

(b) Second shroud $\left(\dfrac{d_s}{d_j} = 1.33\right)$.
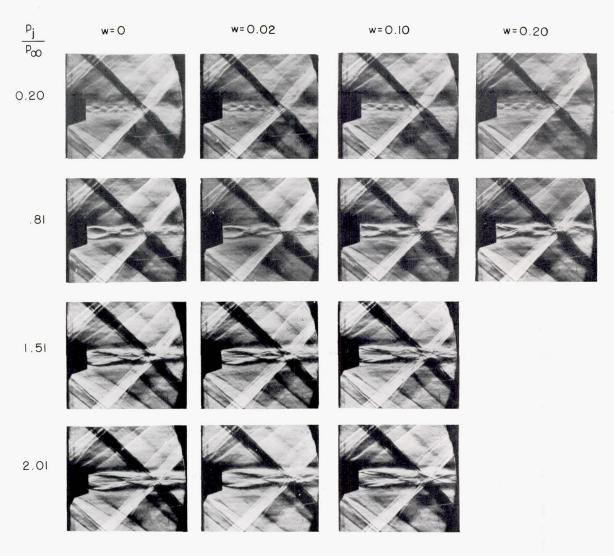
Figure 14.- Concluded.

L-88164

Figure 15.- Typical full-size schlieren photograph illustrating the tunnel flow at a free-stream Mach number of 1.62.

L-88165

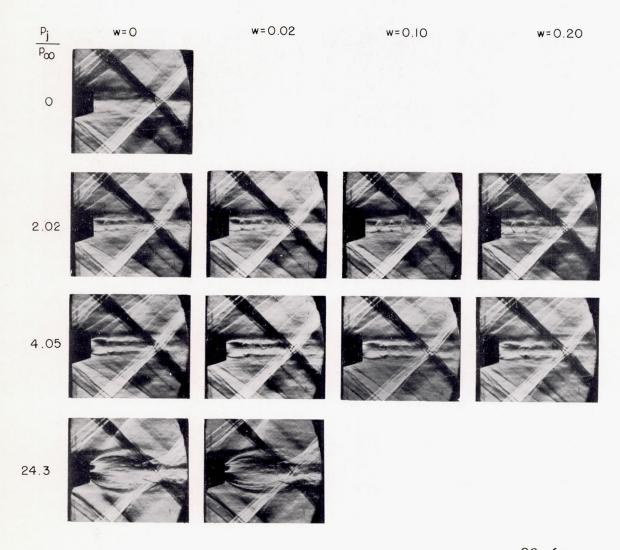(a) First shroud $\left(\dfrac{d_s}{d_j} = 1.50\right)$; supersonic nozzle.

Figure 16.- Schlieren photographs of phenomena associated with primary jet and secondary flow at $M = 1.62$.

(b) Second shroud $\left(\dfrac{d_s}{d_j} = 1.33\right)$; supersonic nozzle.

Figure 16.- Continued.

(c) Second shroud $\left(\dfrac{d_s}{d_j} = 1.33\right)$; sonic nozzle.

L-88167

Figure 16.- Concluded.